

## Biofield Treatment: A Potential Strategy for Modification of Physical and Thermal Properties of Indole

Mahendra Kumar<sup>1</sup>, Rama Mohan<sup>1</sup>, Alice Branton<sup>1</sup>, Dahryn Trivedi<sup>1</sup>, Gopal Nayak<sup>1</sup>, Rakesh K Mishra<sup>2</sup>, and Snehasis Jana<sup>2\*</sup>

<sup>1</sup>Trivedi Global Inc., 10624 S Eastern Avenue Suite A-969, Henderson, NV 89052, USA

<sup>2</sup>Trivedi Science Research Laboratory Pvt. Ltd., Hall-A, Chinar Mega Mall, Chinar Fortune City, Hoshangabad Rd., Bhopal- 462026, Madhya Pradesh, India

### Abstract

Indole compounds are important class of therapeutic molecules, which have excellent pharmaceutical applications. The objective of present research was to investigate the influence of biofield treatment on physical and thermal properties of indole. The study was performed in two groups (control and treated). The control group remained as untreated, and biofield treatment was given to treated group. The control and treated samples were characterized by X-ray diffraction (XRD), differential scanning calorimetry (DSC), thermogravimetric analysis (TGA), Fourier transform infrared (FT-IR) spectroscopy and ultraviolet-visible (UV-Vis) spectroscopy. XRD study demonstrated the increase in crystalline nature of treated indole as compared to control. Additionally, the treated indole showed increase in crystallite size by 2.53% as compared to control. DSC analysis of treated indole (54.45°C) showed no significant change in melting temperature ( $T_m$ ) in comparison with control sample (54.76°C). A significant increase in latent heat of fusion ( $\Delta H$ ) by 30.86% was observed in treated indole with respect to control. Derivative thermogravimetry (DTG) of treated indole showed elevation in maximum thermal decomposition temperature ( $T_{max}$ ) 166.49°C as compared to control (163.37°C). This was due to increase in thermal stability of indole after biofield treatment. FT-IR analysis of treated indole showed increase in frequency of N-H stretching vibrational peak by  $6\text{ cm}^{-1}$  as compared to control sample. UV spectroscopy analysis showed no alteration in absorption wavelength ( $\lambda_{max}$ ) of treated indole with respect to control. The present study showed that biofield has substantially affected the physical and thermal nature of indole.

**Keywords:** Indole; X-ray diffraction; Thermal analysis; Fourier transform infrared spectroscopy; UV-Vis spectroscopy

### Abbreviations

XRD: X-ray diffraction; DSC: Differential scanning calorimetry; TGA: Thermogravimetric analysis; DTA: Differential thermal analyzer; DTG: Derivative thermogravimetry; FT-IR: Fourier transform infrared; UV-Vis: Ultraviolet-visible

### Introduction

The theoretical basis of medicinal chemistry has become much more sophisticated, but is naive to suppose that the discovery of drugs is merely a matter of structure-activity relationships. Indole is organic compound which is parent substance for a large number of important molecules occurring in nature [1]. The indole based compounds are important class of therapeutic molecules which can replace many existing pharmaceuticals in near future. Indole is colourless crystalline solid with a range of odours; naphthalene like in case of indole to fecal in case of skatole (3-methylindole). Tryptophan is an indole derivative which is one of the important amino acids. Especially, serotonin an important indole derivative which is a vasoconstrictor hormone plays an interesting role in conducting impulses to brain [2]. Moreover, some indole alkaloids show significant impact on muscle contraction while toxiferenes act as muscle relaxants. Additionally, 5-hydroxytryptamine receptors an derivative of indole have been used for synthesis of sumatriptan [3] for the treatment of migraine, ondasetran [4] used in chemotherapy, and alosetron [5] for the treatment of irritable bowel syndrome. Delavirdine and inhibitor of cytochrome P450 isozyme CYP3A4, is a drug which has been designed for HIV treatment [6]. Further, indole-3-carbinol (I3C) is a natural indole derivative found commonly in cruciferous vegetables which has been indicated as a promising agent in preventing breast cancer development and progression [7].

Since, indole is used as an intermediate for synthesis of these pharmaceutical compounds, where its rate of reaction plays a pivotal role. In a previous research study it was shown that rate of reaction of an organic compound can be accelerated by increasing its crystallite

size [8]. Hence, by considering the above excellent applications of indole, herein an attempt was made to use an approach that could be beneficial in order to modify the physical and thermal properties of indole.

A physicist, William Tiller proposed the existence of a new force related to human body, in addition to four well known fundamental forces of physics: gravitational force, strong force, weak force, and electromagnetic force. Fritz-Albert, a biophysicist proposed that human physiology shows a high degree of order and stability due to their coherent dynamic states [9-12]. Thus, the human body emits the electromagnetic waves in form of bio-photons, which surrounds the body and it is commonly known as biofield. Therefore, the biofield consists of electromagnetic field, being generated by moving electrically charged particles (ions, cell, molecule etc.) inside the human body. Furthermore, a human has ability to harness the energy from environment/universe and can transmit into any object (living or non-living) around the Globe. The object(s) always receive the energy and respond into useful way that is called biofield energy and this process is known as biofield treatment (The Trivedi Effect®).

Mr. Trivedi's biofield treatment is known to alter the characteristics of many things in several research fields such as, material science [13-17], agriculture [18-20] and biotechnology [21]. Biofield treatment has shown excellent results in improving the antimicrobial susceptibility pattern, and alteration of biochemical reactions, as well as induced alterations in characteristics of pathogenic microbes [22,23]. Exposure

**\*Corresponding author:** Snehasis Jana, Trivedi Science Research Laboratory Pvt. Ltd., Hall-A, Chinar Mega Mall, Chinar Fortune City, Hoshangabad, India, Tel: 91-755-6660006; E-mail: [publication@trivedisrl.com](mailto:publication@trivedisrl.com)

**Received** July 18, 2015; **Accepted** August 03, 2015; **Published** August 10, 2015

**Citation:** Trivedi MK, Tallapragada RM, Branton A, Trivedi D, Nayak G, et al. (2015) Biofield Treatment: A Potential Strategy for Modification of Physical and Thermal Properties of Indole. J Environ Anal Chem 2: 152. doi:10.4172/2380-2391.1000152

**Copyright:** © 2015 Trivedi MK, et al. This is an open-access article distributed under the terms of the Creative Commons Attribution License, which permits unrestricted use, distribution, and reproduction in any medium, provided the original author and source are credited.

to biofield treatment caused paramount increase in medicinal property, growth, and anatomical characteristics of ashwagandha [24].

By considering the above mentioned excellent outcome from biofield treatment and pharmaceutical significance of indole, this study was undertaken to investigate the impact of biofield on its physical and thermal properties.

## Materials and Methods

The indole was procured from S D Fine Chem Pvt. Ltd., India. The control and treated samples were characterized by XRD, DSC, TGA, FT-IR and UV visible analysis.

## Biofield treatment

Indole was divided into two parts; one was kept as a control sample, while the other was subjected to Mr. Trivedi's biofield treatment and coded as treated sample. The treatment group was in sealed pack and handed over to Mr. Trivedi for biofield treatment under laboratory condition. Mr. Trivedi provided the treatment through his energy transmission process to the treated group without touching the sample. After biofield treatment the control and treated group was subjected to physicochemical characterization under standard laboratory conditions.

## Characterization

**X-ray diffraction (XRD) study:** XRD analysis of indole was carried out on Phillips, Holland PW 1710 X-ray diffractometer system, which had a copper anode with nickel filter. The radiation of wavelength used by the XRD system was 1.54056 Å. The data obtained from this XRD were in the form of a chart of  $2\theta$  vs. intensity and a detailed table containing peak intensity counts, d value (Å), peak width ( $\theta$ ), relative intensity (%) etc. The crystallite size (G) was calculated by using formula:

$$G = k\lambda / (b \cos \theta)$$

Here,  $\lambda$  is the wavelength of radiation used, b is full width half maximum (FWHM) of peaks and k is the equipment constant (=0.94). However, percent change in crystallite size was calculated using the following equation:

$$\text{Percent change in crystallite size} = [(G_t - G_c) / G_c] \times 100$$

Where,  $G_c$  and  $G_t$  are crystallite size of control and treated powder samples respectively.

## Differential scanning calorimetry (DSC) study

The control and treated indole were analyzed by using a Pyris-6 Perkin Elmer DSC on a heating rate of 10°C/min under air atmosphere and air was flushed at a flow rate of 5 mL/min.

Percent change in melting point was calculated using following equations:

$$\% \text{ change in Melting point} = \frac{[T_{\text{Treated}} - T_{\text{control}}]}{T_{\text{control}}} \times 100$$

Where,  $T_{\text{Control}}$  and  $T_{\text{Treated}}$  are the melting point of control and treated samples, respectively.

Percent change in latent heat of fusion was calculated using following equations:

$$\% \text{ change in Latent heat of fusion} = \frac{[\Delta T_{\text{Treated}} - \Delta T_{\text{control}}]}{\Delta T_{\text{control}}} \times 100$$

Where,  $\Delta H_{\text{Control}}$  and  $\Delta H_{\text{Treated}}$  are the latent heat of fusion of control

and treated samples, respectively.

## Thermogravimetric analysis-differential thermal analysis (TGA-DTA)

Thermal stability of control and treated indole were analyzed by using Mettler Toledo simultaneous TGA and Differential thermal analyzer (DTA). The samples were heated from room temperature to 400°C with a heating rate of 5°C/min under air atmosphere.

Percent change in temperature at which maximum weight loss occur in sample was calculated using following equation:

$$\% \text{ change in } T_{\text{max}} = \left[ \frac{(T_{\text{max, treated}} - T_{\text{max, control}})}{T_{\text{max, control}}} \right] \times 100$$

Where,  $T_{\text{max, control}}$  and  $T_{\text{max, treated}}$  are the maximum thermal decomposition temperature in control and treated sample, respectively.

## FT-IR spectroscopy

FT-IR spectra were recorded on Shimadzu's Fourier transform infrared spectrometer (Japan) with frequency range of 4000-500  $\text{cm}^{-1}$ . The treated sample was divided in two parts T1 and T2 for FTIR analysis.

**Uv-Vis spectroscopic analysis:** UV spectra of control and treated indole were recorded on Shimadzu UV-2400 PC series spectrophotometer with 1 cm quartz cell and a slit width of 2.0 nm. The analysis was carried out using wavelength in the range of 200-400 nm. The treated sample was divided in two parts T1 and T2 for the analysis.

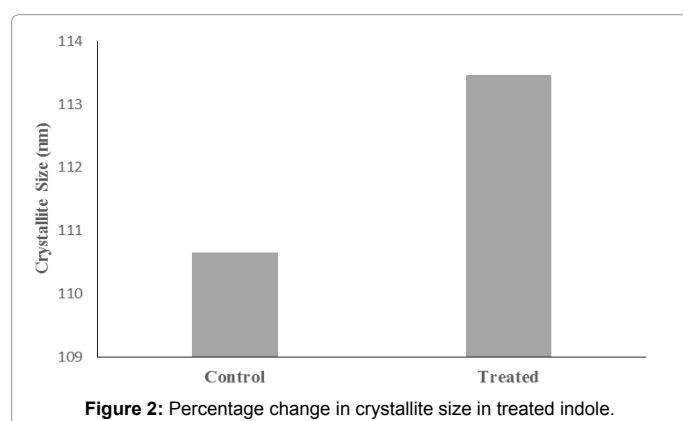
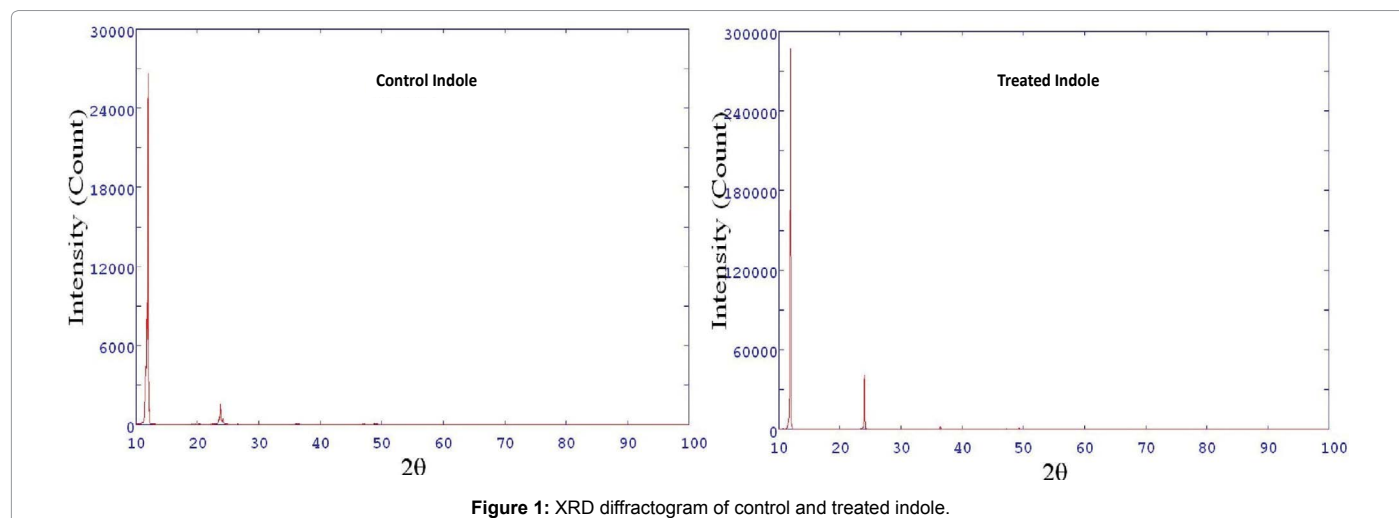
## Results and Discussion

### XRD characterization

XRD of control and treated indole are presented in Figure 1. The control indole showed the XRD peaks at  $2\theta$  equals to 11.42°, 11.55°, 11.81°, 11.99°, 12.19°, 23.55°, 23.78°, 24.15° and 49.23°. Whereas the treated indole XRD diffractogram showed increase in intensity of the peaks. The XRD showed peaks at  $2\theta$  equals to 10.76°, 11.59°, 11.93°, 12.20°, 20.31°, 21.68°, 24.03°, 36.41°, 36.52°, 47.24°, 47.40°, and 49.26°. The increase in intensity of the biofield treated indole may be attributed to increase in long range order of the atoms. The crystallite size was calculated using Scherrer formula ( $\text{crystallite size} = k\lambda / b \cos \theta$ ) and the result are presented in Figure 2. The control indole showed a crystallite size 110.65 nm; however, the treated showed increase in crystallite size (113.46 nm). The crystallite size was increased by 2.53% as compared to control indole. Caruntu et al., showed uniform increase in crystallite size with increasing sintering temperature [25]. Gaber et al., showed that elevation in processing temperature caused decrease in dislocation density and increase in number of unit cell which ultimately increased the crystal growth [26]. Additionally, Raj et al., also suggested that increase in temperature causes drastic increase in particle size due to aggregation followed by increase in crystallite size [27]. They suggested that increase in temperature caused depression in the thermodynamically driven force which led to decrease in nuclear densities and thus increase in crystallite size [28-29]. Hence, it is assumed that biofield treatment may cause decrease in nuclear density that led to increase in crystallite size. Carballo et al., reported that rate of reaction can be significantly improved by increase in crystallite size [8]. Hence, treated indole due to high crystallite size may improve the reaction rate and percentage yield during synthesis of pharmaceutical compounds.

### DSC Characterization

DSC was used to investigate the melting temperature and latent heat of fusion of control and treated indole. DSC thermogram of control indole showed melting temperature peak at 54.76°C (Figure



3). However, the DSC of treated indole showed a melting temperature peak at 54.45°C. The change in melting temperature of treated indole as compared to control was 0.56%. The result showed that there was no significant change in melting temperature of treated indole as compared to control. It may be inferred that biofield did not influence the melting process of the treated indole. The latent heat of fusion of control indole was 92.41 J/g; however, the treated sample showed increase in latent heat of fusion (120.93 J/g) (Table 1). The increase in latent heat of fusion was 30.86% in treated indole as compared to control. In a solid, substantial amount of interaction force exists in atomic bonds to hold the atoms at their positions, thus a sufficient amount of energy is required to change the phase from solid to liquid, known as latent heat of fusion ( $\Delta H$ ). Further, the energy supplied during phase change i.e.  $\Delta H$  is stored as potential energy of atoms [30]. Hence, it is assumed that biofield treatment may altered the potential energy of treated indole as compared to control that led to increase in latent heat of fusion.

### TGA analysis

TGA thermogram of control and treated Indole are presented in Figures 4 and 5, respectively. The thermogram of control indole showed one step thermal degradation pattern. The sample started to thermally degrade at around 147°C and this process terminated at around 185°C. The control sample lost 46.52% of its weight during this step. Whereas the treated indole also showed one step thermal degradation. The thermal degradation commenced at around 150°C and degradation terminated at around 189°C. During this step the treated indole lost

55.53% of its weight.

DTA thermograms of control and treated indole are shown in Figures 4 and 5, respectively. The control sample showed a broad endothermic peak at 174.12°C may be due to decomposition of the sample. However, the treated indole showed slight elevation in this temperature and it was observed at 176.97°C. The DTG thermogram of control indole showed (Table 1)  $T_{max}$  value at 163.37°C; however, it was increased to 166.49°C in treated indole. The  $T_{max}$  was increased by 1.90% in treated indole as compared to control. This increase in  $T_{max}$  of treated indole showed the higher thermal stability as compared to control. Szabo et al., showed that thermal stability of poly (hexadecylthiophene) increased after radiation treatment. They suggested that conformational changes in side alkyl and crosslinking causes elevation in thermal stability [31]. Hence, it is presumed that biofield treatment may induce crosslinking in treated indole molecules which lead to increase in thermal stability.

### FT-IR Spectroscopy

FT-IR spectrum of control indole is presented in Figure 6. The typical FT-IR of control indole showed stretching vibration band at 3406  $\text{cm}^{-1}$  which was attributed to the N-H peak. The peak at 3022  $\text{cm}^{-1}$  and 3049  $\text{cm}^{-1}$  can be attributed to symmetric and asymmetric C-H stretching vibration peaks. The characteristic aromatic C=C strong stretching were appeared at 1508  $\text{cm}^{-1}$ , and 1577  $\text{cm}^{-1}$  in the sample. Vibrations peaks at 1616  $\text{cm}^{-1}$ , and 1456  $\text{cm}^{-1}$  were due to C-C (in ring) stretching in the sample. Other important peaks were observed at 1336  $\text{cm}^{-1}$  and, 1352  $\text{cm}^{-1}$  due to C-H bending modes of symmetric and asymmetric methyl groups. Vibration peaks at 609  $\text{cm}^{-1}$ , 731  $\text{cm}^{-1}$  and 744  $\text{cm}^{-1}$  appeared due =C-H bending peaks in control. The FT-IR region below 1000  $\text{cm}^{-1}$  exhibits the out of plane bending of C-H bond vibrations of aromatic carbon double bonds. The observed FT-IR data is well supported from reported literature [32].

FT-IR spectrum of treated indole (T1 and T2) are presented in Figure 7. The FT-IR spectrum of T1 showed important peaks at 3404  $\text{cm}^{-1}$  and 3049  $\text{cm}^{-1}$  which were due to N-H and C-H stretching vibration peaks. The C=C aromatic stretching vibration peaks were observed at 1504  $\text{cm}^{-1}$  and 1577  $\text{cm}^{-1}$ . The stretching vibration bands for C-C peak appeared at 1413  $\text{cm}^{-1}$ , 1477  $\text{cm}^{-1}$  and 1614  $\text{cm}^{-1}$ . Vibrations bands at 1336  $\text{cm}^{-1}$  and 1352  $\text{cm}^{-1}$  were due to C-H bending modes of symmetric and asymmetric methyl groups. The T1 showed another stretching peaks at 611  $\text{cm}^{-1}$ , 729  $\text{cm}^{-1}$ , and 746  $\text{cm}^{-1}$  which were mainly due to =C-H bending vibrations.

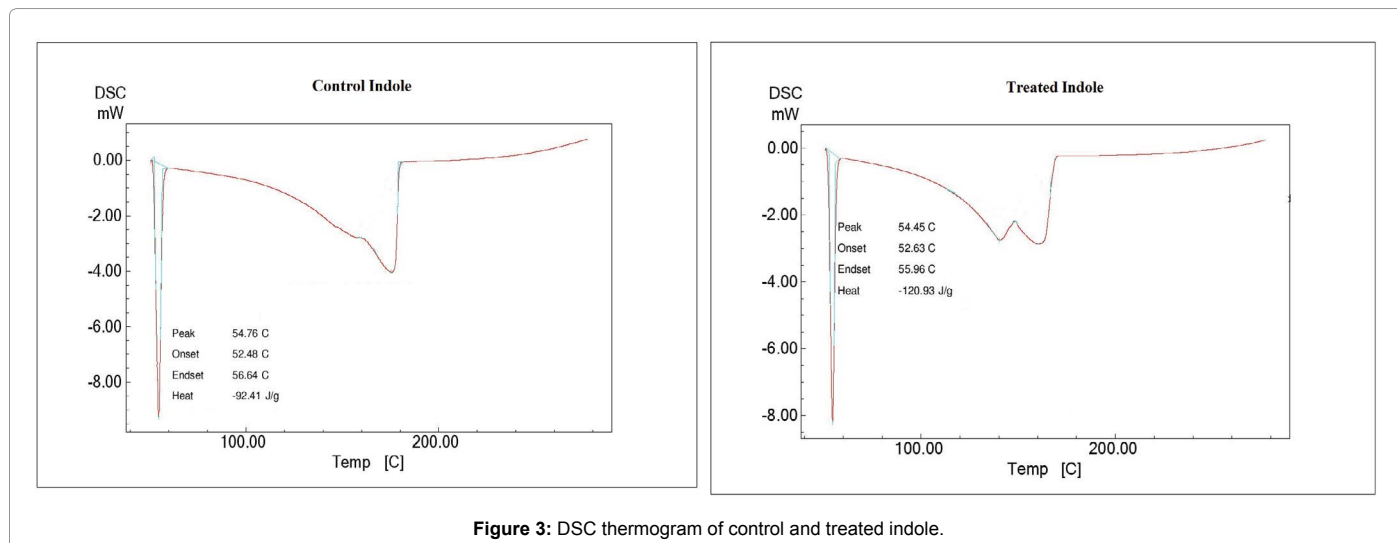


Figure 3: DSC thermogram of control and treated indole.

Sample	T <sub>m</sub> (°C; control)	T <sub>m</sub> (°C; treated)	% Change in T <sub>m</sub> (°C)	Control (ΔH J/g)	Treated (ΔH J/g)	% Change in ΔH	T <sub>max</sub> (°C; control)	T <sub>max</sub> (°C; treated)	% Change in T <sub>max</sub>
Indole	54.76	54.45	-0.56	-92.41	-120.93	30.86	163.37	166.49	1.90

Table 1: Thermal analysis data of control and treated indole.

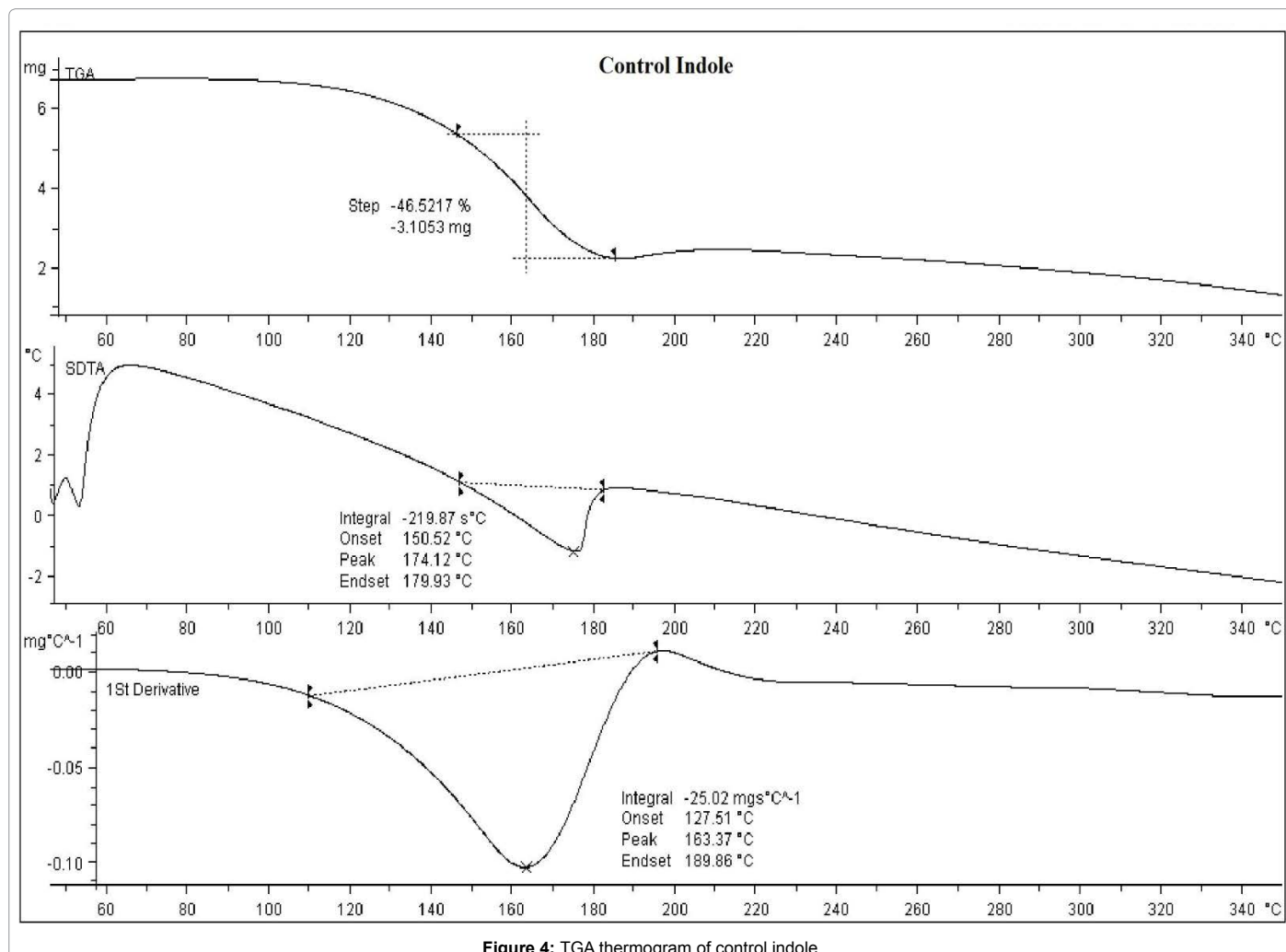


Figure 4: TGA thermogram of control indole.

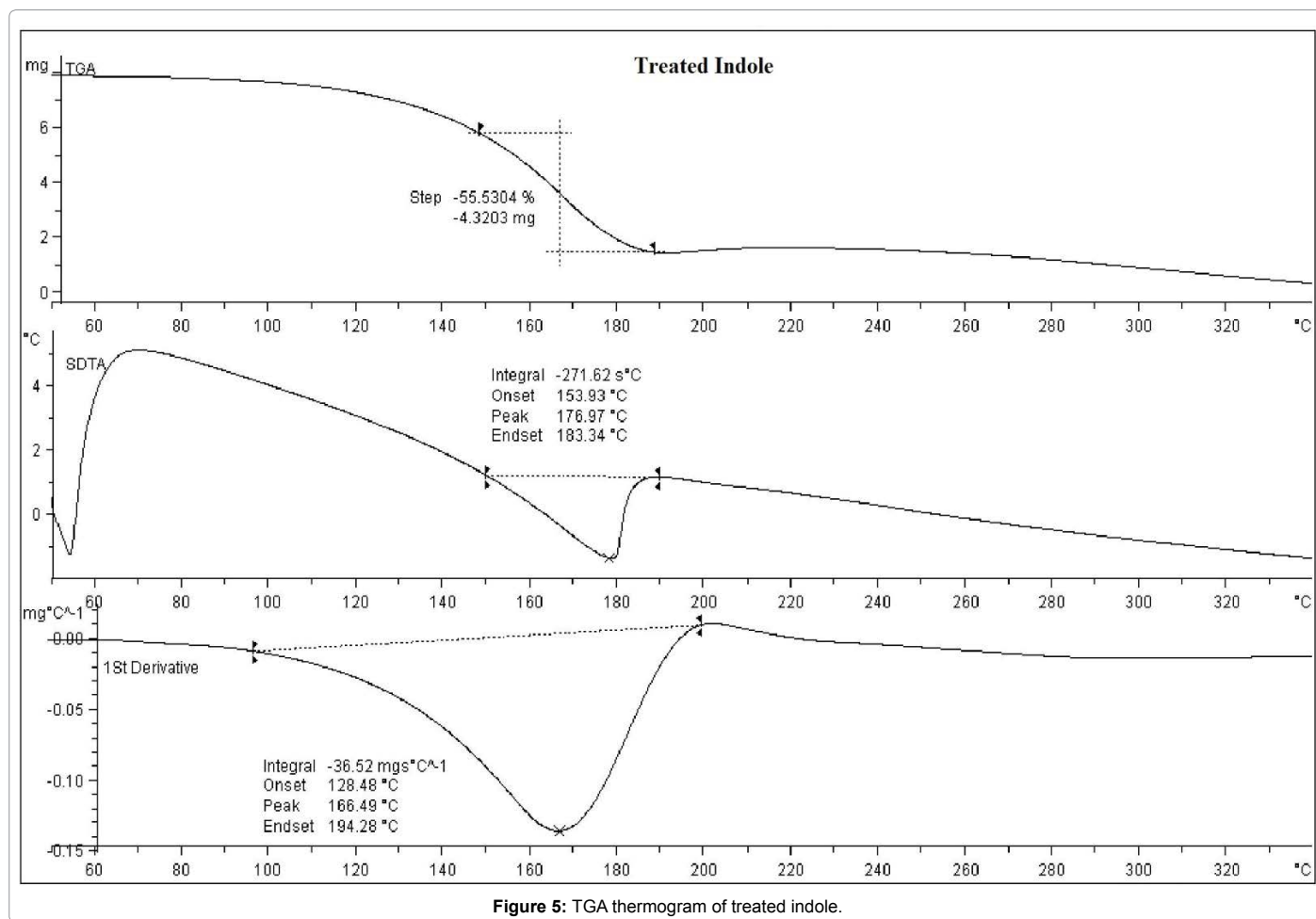


Figure 5: TGA thermogram of treated indole.

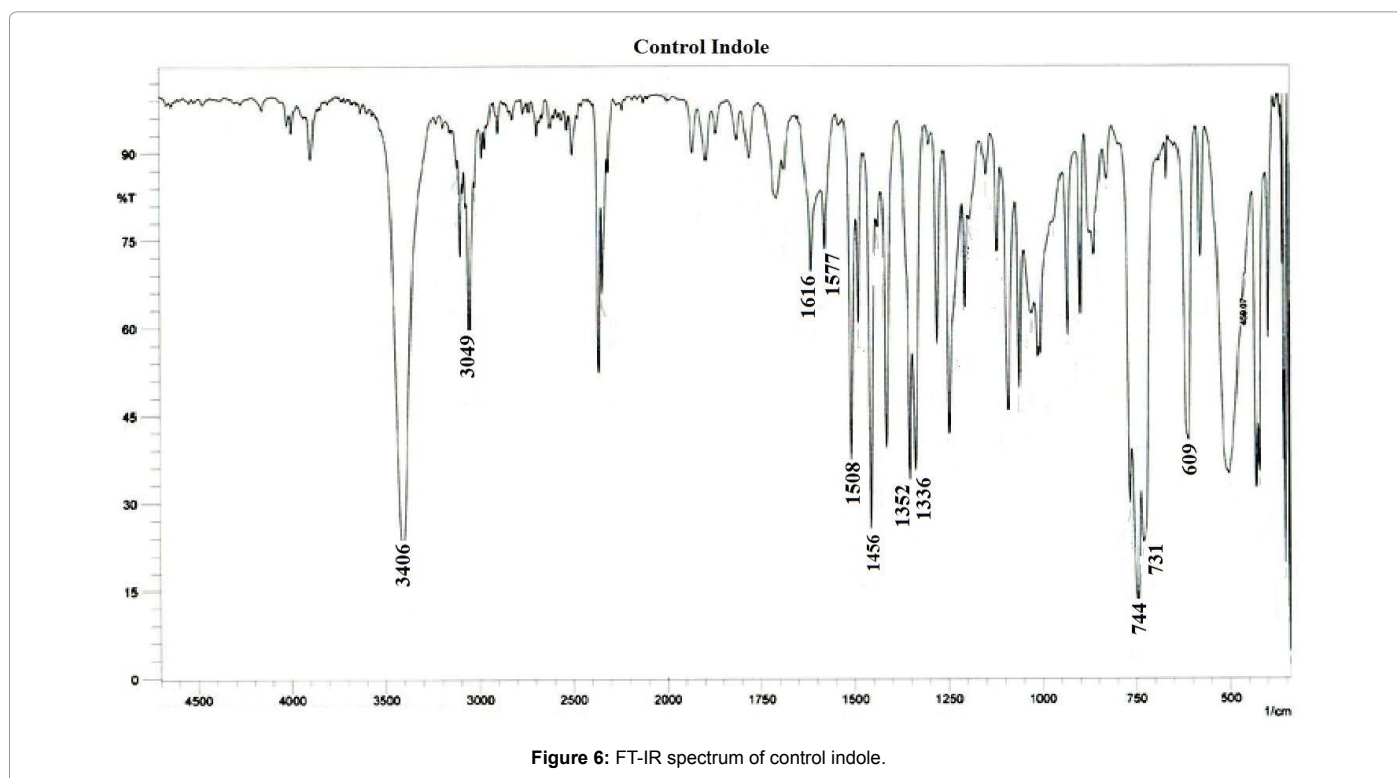


Figure 6: FT-IR spectrum of control indole.

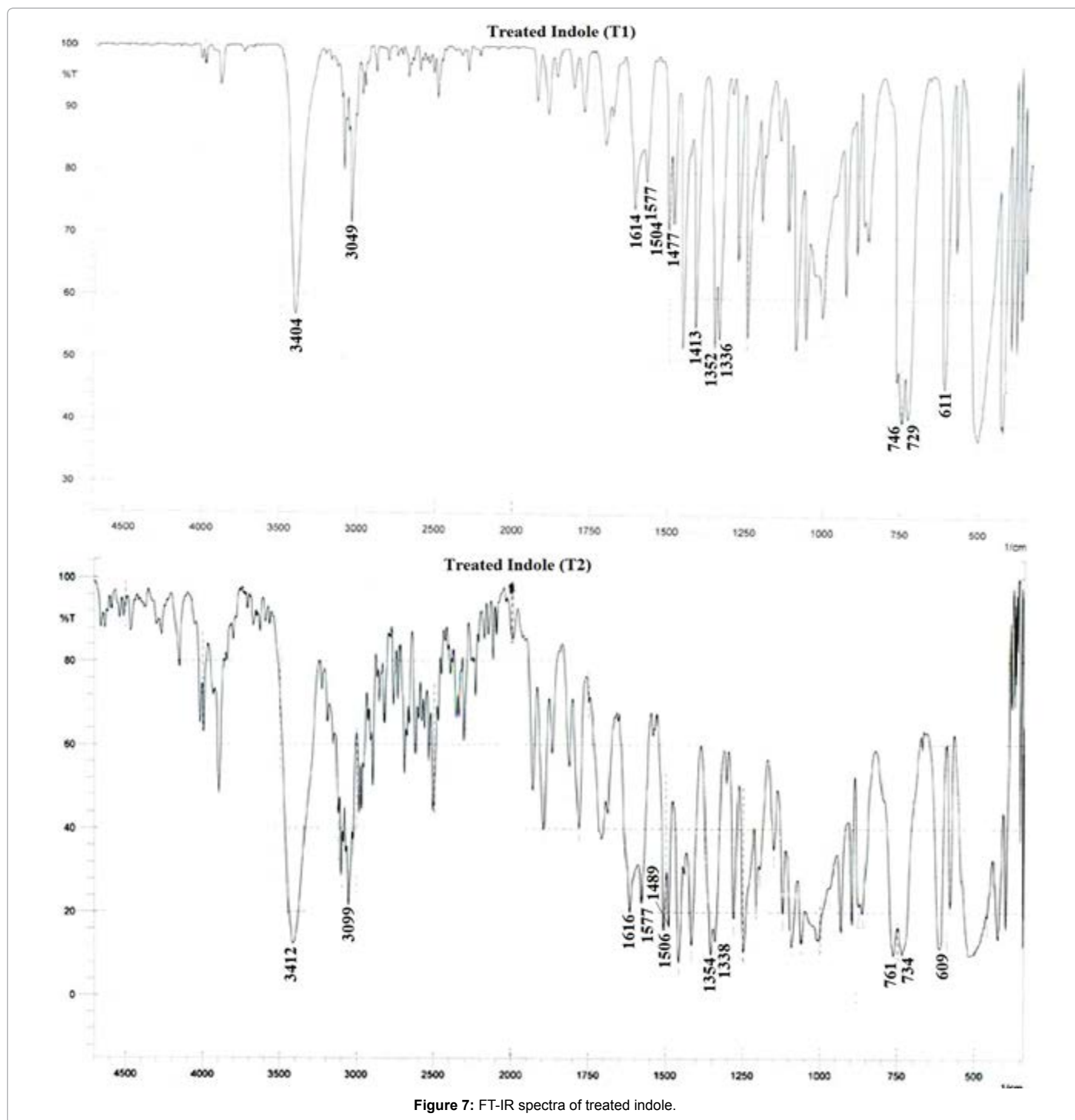


Figure 7: FT-IR spectra of treated indole.

The FTIR spectrum of T2 showed stretching vibration peaks for C-H aromatics at  $3099\text{ cm}^{-1}$ . The C=C stretching peaks were appeared at  $1506\text{ cm}^{-1}$  and  $1577\text{ cm}^{-1}$ . Vibrations bands at  $1338\text{ cm}^{-1}$  and  $1354\text{ cm}^{-1}$  were due to C-H bending modes of symmetric and asymmetric methyl groups. Vibrations bands at  $1489\text{ cm}^{-1}$  and  $1616\text{ cm}^{-1}$  were due to C-C (in ring) stretching in the sample. Other important peaks were appeared at  $609\text{ cm}^{-1}$ ,  $734\text{ cm}^{-1}$  and  $761\text{ cm}^{-1}$  due to =C-H bending vibration peaks. Whereas, the FT-IR spectrum of T2 showed increase in N-H stretching vibration peak at  $3412\text{ cm}^{-1}$  which may be due to increase force constant and stability of the bond. It was previously

suggested that increase in frequency of any bond causes possible enhancement in force constant of respective bond [33].

#### UV visible spectroscopy

The UV spectra of control and treated indole (T1 and T2) are shown in Figures 8 and 9, respectively. The UV spectrum of control indole showed two main absorption peaks *i.e.* at 217 and 287 nm ( $\lambda_{\text{max}}$ ) and the spectrum is well supported with the literature [34]. Similarly, the treated indole (T1) also showed absorption peaks at 216 and 287 nm. Whereas the treated indole (T2) also showed absorption peaks at 216 and 287 nm. It suggests

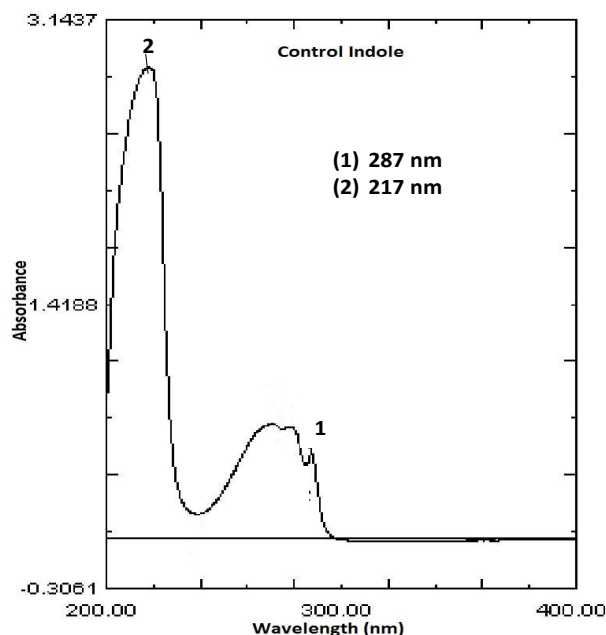


Figure 8: UV spectrum of control indole.

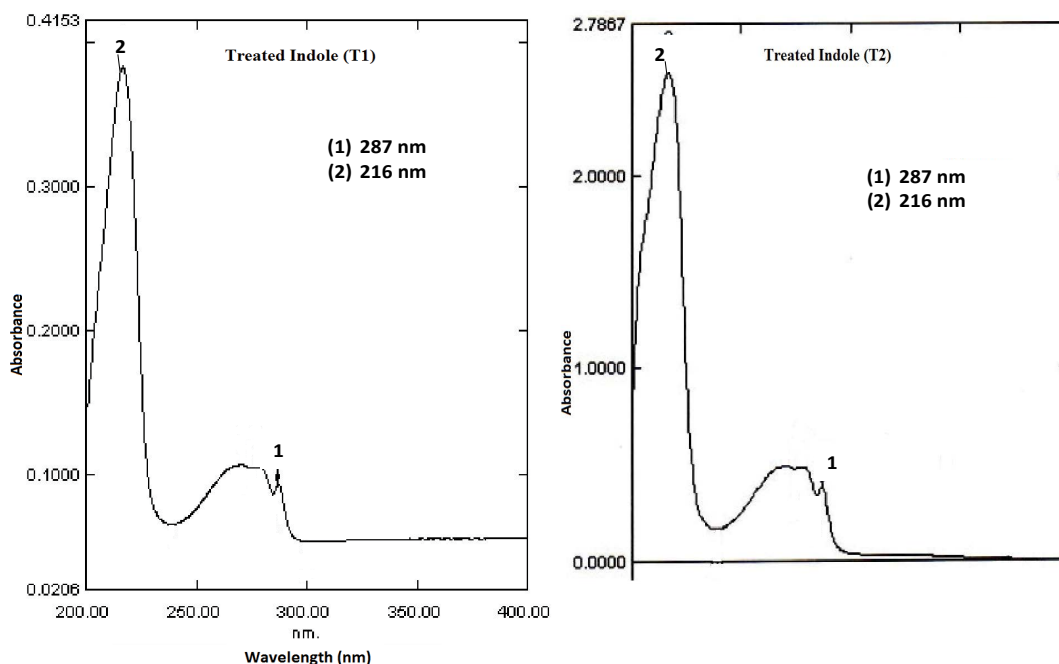


Figure 9: UV spectra of treated indole).

that biofield treatment did not make any alteration in chromophore groups of treated indole sample as compared to control.

## Conclusion

The study results showed the significant impact of biofield treatment on physical and thermal properties of indole. XRD data on treated indole showed an increase in crystallite size with respect to control sample. It is presumed that decrease in nuclear density may cause increase in crystallite size. DSC analysis of treated indole showed no change in melting temperature as compared to control.

Additionally, latent heat of fusion was substantially increased by 30.86% in treated indole as compared to control. TGA analysis of treated indole showed enhanced thermal stability as compared to control sample. FTIR data showed increase in force constant and stability of the N-H bond of treated indole as compared to control. The enhanced crystallite size and high thermal stability of treated indole may improve the reaction rate. Hence, it is assumed that biofield treated indole could be used as intermediate for synthesis of pharmaceutical compounds.

## Acknowledgement

The authors would like to thank Trivedi Science, Trivedi Master Wellness and Trivedi Testimonials for their support during the work. The authors would like to also thank all the laboratory staff of MG V Pharmacy College, Nashik for their assistance during the various instrument characterizations.

## References

1. Radwanski ER, Last RL (1995) Tryptophan biosynthesis and metabolism: biochemical and molecular genetics. *Plant Cell* 7: 921-934.
2. Berger M, Gray JA, Roth BL (2009) The expanded biology of serotonin. *Annu Rev Med* 60: 355-366.
3. Freidank-Mueschenborn E, Fox AW (2005) Resolution of concentration-response differences in onset of effect between subcutaneous and oral sumatriptan. *Headache* 45: 632-637.
4. Generali JA, Cada DJ (2009) Off-label drug uses-Ondansetron: Postanesthetic shivering. *Hosp Pharm* 44: 670-671.
5. Horton R (2001) Lotronex and the FDA: a fatal erosion of integrity. *Lancet* 357: 1544-1545.
6. Scott LJ, Perry CM (2000) Delavirdine: a review of its use in HIV infection. *Drugs* 60: 1411-1444.
7. Meng Q, Qi M, Chen DZ, Yuan R, Goldberg ID, et al. (2000) Suppression of breast cancer invasion and migration by indole-3-carbinol: associated with up-regulation of BRCA1 and E-cadherin/catenin complexes. *J Mol Med (Berl)* 78: 155-165.
8. Carballo LM, Wolf EE (1978) Crystallite size effects during the catalytic oxidation of propylene on Pt/ $\gamma$ -Al<sub>2</sub>O<sub>3</sub>. *J Catal* 53: 366-373.
9. Popp FA, Chang JJ, Herzog A, Yan Z, Yan Y (2002) Evidence of non-classical (squeezed) light in biological systems. *Phys Lett* 293: 98-102.
10. Popp FA, Quao G, Ke-Hsuen L (1994) Biophoton emission: experimental background and theoretical approaches. *Mod Phys Lett B* 8: 21-22.
11. Popp FA (1992) Recent advances in biophoton research and its application. World Scientific Publishing Co. Pvt. Ltd.
12. Cohen S, Popp FA (2003) Biophoton emission of human body. *Indian J Exp Biol* 41: 440-445.
13. Trivedi MK, Patil S, Tallapragada RM (2013) Effect of biofield treatment on the physical and thermal characteristics of vanadium pentoxide powders. *J Material Sci Eng S11*: 001.
14. Trivedi MK, Patil S, Tallapragada RM (2013) Effect of biofield treatment on the physical and thermal characteristics of silicon, tin and lead powders. *J Material Sci Eng* 2: 125.
15. Trivedi MK, Patil S, Tallapragada RM (2014) Atomic, crystalline and powder characteristics of treated zirconia and silica powders. *J Material Sci Eng* 3: 144.
16. Trivedi MK, Patil S, Tallapragada RMR (2015) Effect of biofield treatment on the physical and thermal characteristics of aluminium powders. *Ind Eng Manag* 4: 151.
17. Trivedi MK, Nayak G, Patil S, Tallapragada RM, Latiyal O (2015) Studies of the atomic and crystalline characteristics of ceramic oxide nano powders after bio field treatment. *Ind Eng Manage* 4: 161.
18. Shinde V, Sances F, Patil S, Spence A (2012) Impact of biofield treatment on growth and yield of lettuce and tomato. *Aust J Basic Appl Sci* 6: 100-105.
19. Sances F, Flora E, Patil S, Spence A, Shinde V (2013) Impact of biofield treatment on ginseng and organic blueberry yield. *Agrivita J Agric Sci* 35: 22-29.
20. Lenssen AW (2013) Biofield and fungicide seed treatment influences on soybean productivity, seed quality and weed community. *Agricultural Journal* 8: 138-143.
21. Patil SA, Nayak GB, Barve SS, Tembe RP, Khan RR (2012) Impact of biofield treatment on growth and anatomical characteristics of *Pogostemon cablin* (Benth.). *Biotechnology* 11: 154-162.
22. Trivedi MK, Patil S, Shettigar H, Gangwar M, Jana S (2015) Antimicrobial sensitivity pattern of *Pseudomonas fluorescens* after biofield treatment. *J Infect Dis Ther* 3: 222.
23. Trivedi MK, Patil S, Shettigar H, Bairwa K, Jana S (2015) Phenotypic and biotypic characterization of *Klebsiella oxytoca*: An impact of biofield treatment. *J Microb Biochem Technol* 7: 203-206.
24. Altekar N, Nayak G (2015) Effect of biofield treatment on plant growth and adaptation. *J Environ Health Sci* 1: 1-9.
25. Caruntu G, Rarig Jr R, Dumitru I, O'Connor CJ (2006) Annealing effects on the crystallite size and dielectric properties of ultrafine Ba<sub>1-x</sub>Sr<sub>x</sub>TiO<sub>3</sub> (0 < x < 1) powders synthesized through an oxalate-complex precursor. *J Mater Chem* 16: 752-758.
26. Gaber A, Abdel-Rahim MA, Abdel-Latif AY, Abdel-Salam MN (2014) Influence of calcination temperature on the structure and porosity of nanocrystalline SnO<sub>2</sub> synthesized by a conventional precipitation method. *Int J Electrochem Sci* 9: 81-95.
27. Raj KJA, Viswanathan B (2009) Effect of surface area, pore volume, particle size of P25 titania on the phase transformation of anatase to rutile. *Indian J Chem* 48A: 1378-1382.
28. Rashidi AM, Amadeh A (2009) The effect of saccharin addition and bath temperature on the grain size of nanocrystalline nickel coatings. *Surf Coat Technol* 204: 353-358.
29. Gusain D, Srivastava V, Singh VK, Sharma YC (2014) Crystallite size and phase transition demeanor of ceramic steel. *Mater Chem Phys* 145: 320-326.
30. Moore J (2010) Chemistry: The molecular science (4th edn) Brooks Cole.
31. Szabo L, Cik G, Lensy J (1996) Thermal stability increase of doped poly (3-hexadecylthiophene) by  $\gamma$ -radiation. *Synt Met* 78: 149-153.
32. Vazquez-Vuelvas OF, Hernandez-Madriral JV, Gavino R, Tlenkopatchev MA, Morales DM, et al. (2011) X-ray, DFT, FTIR and NMR structural study of 2,3-dihydro-2-(R-phenylacylidene)-1,3,3-trimethyl-1H-indole. *J Mol Struct* 987: 106-118.
33. Pavia DL, Lampman GM, Kriz GS (2001) Introduction to spectroscopy. (3rd edn), Thomson learning, Singapore.
34. van der Geer EPL, Li Q, van Koten G, Klein Gebbink RJM, Hessen B (2008) N-Substituted indole-3-thiolate [4Fe-4S] clusters with a unique and tunable combination of spectral and redox properties. *Inorg Chim Acta* 361: 1811-1818.